

RESEARCH PAPER

Therapeutic Potential of *Selenicereus Undatus* Nanoemulsion Against Breast Cancer: A Comprehensive Analysis of Antitumor Activity, Oxidative Stress Modulation, and Antimicrobial Properties

Ahmed Habeeb Almamoori ^{1,2}, Latifeh Pourakbar ¹, Jalil Khara ^{1*} and Ali H. Al-Marzoqi ^{2*}

¹ Department of Biology, Faculty of Sciences, Urmia University, Urmia, Iran

² College of Science for Women, Babylon University, Iraq

ARTICLE INFO

Article History:

Received 04 January 2025

Accepted 23 February 2026

Published 01 April 2026

Keywords:

Antioxidant

Breast cancer

Gene expression

Nanoemulsion

Selenicereus undatus

ABSTRACT

This study investigates the therapeutic potential of *Selenicereus undatus* nanoemulsion (NE-SU) as a novel treatment modality for breast cancer, incorporating comprehensive analyses of its anticancer, antioxidant, and antimicrobial properties. The nanoemulsion was successfully formulated and characterized through dynamic light scattering for particle size analysis, demonstrating a bimodal size distribution (21.2 nm and 103 nm). Chemical characterization through GC-MS of the plant extract revealed predominant bioactive compounds including tetradecanoic and hexadecanoic acids. In vitro studies demonstrated dose-dependent cytotoxicity against MCF-7 breast cancer cells with an IC₅₀ of 81.09 µg/ml, while flow cytometry analysis revealed significant apoptosis induction (52.11 ± 2.092%) at 80 µg/ml. The nanoemulsion exhibited potent DPPH radical scavenging activity (95.37 ± 0.6997% at 320 µg/ml), comparable to vitamin C. In vivo studies using a 4T1 breast cancer mouse model showed significant tumor growth inhibition, with high-dose treatment (200 mg/kg) reducing tumor size by approximately 59% after four weeks. Molecular analyses revealed significant upregulation of pro-apoptotic genes (*BAX*: 3.519-fold, *Caspase-3*: 2.343-fold) and downregulation of anti-apoptotic *BCL2* (0.3208-fold). The treatment modulated oxidative stress parameters and demonstrated notable antimicrobial activity against *Escherichia coli* and *Pseudomonas aeruginosa*. Histopathological examination confirmed therapeutic efficacy through increased tumor necrosis (36.62 ± 5.828%) in treated groups. These findings establish NE-SU as a promising therapeutic agent with multiple mechanisms of action, suggesting potential applications in cancer treatment strategies.

How to cite this article

Almamoori, Pourakbar L., Khara J. Al-Marzoqi A. Therapeutic Potential of *Selenicereus Undatus* Nanoemulsion Against Breast Cancer: A Comprehensive Analysis of Antitumor Activity, Oxidative Stress Modulation, and Antimicrobial Properties. J Nanostruct, 2026; 16(2):1626-1642. DOI: 10.22052/JNS.2026.02.015

INTRODUCTION

Breast cancer remains the most frequently diagnosed malignancy among women globally,

* Corresponding Author Email: j.khara@urmia.ac.ir

with approximately 2.3 million new cases reported in 2020 alone, accounting for 11.7% of all cancer diagnoses [1]. Statistical analyses



This work is licensed under the Creative Commons Attribution 4.0 International License.

To view a copy of this license, visit <http://creativecommons.org/licenses/by/4.0/>.

indicate a concerning trend, with incidence rates increasing by approximately 0.3% annually over the past decade in developed nations [2]. Despite significant advances in conventional therapeutic approaches, including surgical interventions, chemotherapy protocols, and targeted radiation treatments, breast cancer continues to be the leading cause of cancer-related mortality among women worldwide, with an estimated 685,000 deaths recorded in 2020 [3].

The limitations of current therapeutic modalities are particularly evident in the treatment outcomes of aggressive breast cancer subtypes [4]. Triple-negative breast cancer, representing approximately 15-20% of all breast cancer cases, demonstrates particularly poor prognosis with a median survival of 13.3 months in metastatic cases [5]. Conventional chemotherapeutic agents, notably doxorubicin, while showing initial efficacy with response rates of 40-60%, are associated with severe adverse effects including dose-dependent cardiotoxicity affecting up to 26% of treated patients [6]. These limitations have created an urgent need for alternative therapeutic strategies that can effectively target cancer cells while minimizing damage to healthy tissues [6].

Natural compounds have emerged as promising candidates in cancer therapy, with approximately 60% of currently approved anticancer drugs derived from or inspired by natural sources. *Selenicereus undatus*, commonly known as dragon fruit (formerly known as *Hylocereus undatus*), has attracted significant scientific attention due to its rich phytochemical profile. This climbing cactus, native to the Americas but now cultivated worldwide, has been traditionally used in various medicinal applications across different cultures [7]. Recent analytical studies have revealed substantial concentrations of bioactive compounds, with polyphenolic content ranging from 86.2 to 118.4 mg GAE/100g fresh weight, and flavonoid concentrations of 8.7 to 11.5 mg CE/100g fresh weight. These compounds demonstrate remarkable antioxidant capacity, with DPPH radical scavenging activity reaching 83.7% at concentrations of 100 µg/mL anti-inflammatory, and potential anticancer properties [8, 9].

The therapeutic potential of *S. undatus* is particularly intriguing in the context of cancer treatment, as its constituents have demonstrated multiple mechanisms of action that could be beneficial in targeting cancer cells [10]. These

include the modulation of oxidative stress, regulation of apoptotic pathways, and potential immunomodulatory effects [11]. However, the application of natural compounds in cancer therapy often faces challenges related to bioavailability, stability, and targeted delivery to cancer cells [12].

To address these limitations, the development of nanoemulsion-based delivery systems has emerged as a promising strategy. Nanoemulsions offer several advantages, including improved solubility of hydrophobic compounds, enhanced cellular uptake, and the potential for targeted delivery to cancer cells [13]. These nanoformulations can protect bioactive compounds from degradation while potentially enhancing their therapeutic efficacy through improved biodistribution and cellular penetration [14].

The integration of *S. undatus* extracts into nanoemulsion systems represents an innovative approach to potentially enhance their anticancer efficacy. Recent studies have demonstrated that natural compound-based nanoemulsions can significantly improve the delivery and efficacy of bioactive components while potentially reducing systemic toxicity [15]. The nano-scale size of these formulations facilitates enhanced permeability and retention (EPR) effects in tumor tissues, potentially leading to improved therapeutic outcomes [16]. Additionally, nanoemulsions can protect sensitive bioactive compounds from degradation while potentially enhancing their bioavailability and cellular uptake. [17]

The development of resistance to conventional chemotherapeutic agents remains a significant challenge in breast cancer treatment. This resistance often involves multiple mechanisms, including increased expression of anti-apoptotic proteins, enhanced drug efflux, and altered cellular metabolism [18, 19]. Natural compounds, particularly when delivered via advanced delivery systems like nanoemulsions, may offer advantages in this context by targeting multiple cellular pathways simultaneously, potentially reducing the likelihood of resistance development [20].

Furthermore, the potential antimicrobial properties of *S. undatus* extracts add another dimension to their therapeutic potential. Cancer patients, particularly those undergoing chemotherapy, are often at increased risk of infections due to compromised immune systems. The development of therapeutic agents that

combine anticancer and antimicrobial properties could provide additional benefits in the clinical management of cancer patients [21, 22].

Therefore, this study aimed to evaluate the therapeutic potential of *S. undatus* nanoemulsion against breast cancer through multiple investigative approaches. The specific objectives included: (1) developing and characterizing a stable nanoemulsion formulation of *S. undatus* extract, (2) assessing its anticancer efficacy through in vitro and in vivo studies, (3) elucidating the molecular mechanisms underlying its therapeutic effects, particularly focusing on apoptotic pathways and oxidative stress modulation, and (4) investigating its potential antimicrobial properties as a complementary therapeutic benefit. This comprehensive evaluation was designed to establish the potential of *S. undatus* nanoemulsion as a novel therapeutic agent for breast cancer treatment.

MATERIALS AND METHODS

Plant Material and Authentication

Selenicereus undatus (previously *Hylocereus undatus*) plant material was procured from local markets in Babylon, Iraq. Taxonomic authentication and species verification were conducted at the Herbarium of Urmia University, Iran, where the genus and species were confirmed and documented. The stem bark was separated, thoroughly washed with distilled water, chopped into small pieces, and air-dried at 70°C for 24 hours using a drying oven (Shimiazma, Iran). The dried material was ground to a uniform particle size of 0.25 mm and stored appropriately until further use.

Extract Preparation and Nanoemulsion Formulation

The hydro-alcoholic extract was prepared by soaking 100 g of the processed *S. undatus* stem bark in 500 ml of absolute ethanol for 72 hours at room temperature. The extract was filtered through filter paper and concentrated using a rotary evaporator. The nanoemulsion (NE-SU) was formulated by combining 1% w/w herbal extract with soybean oil (1%) and Tween 80 (40%) dissolved in deionized water. The aqueous phase was gradually added to the oil phase at 2 ml/min under ultrasonic homogenization at room temperature ($28 \pm 2^\circ\text{C}$), maintaining a 45:55 aqueous to oil phase ratio. Homogenization

continued for 15 minutes after complete phase addition.

Particle Size Analysis

Particle size distribution of the nanoemulsion was analyzed using dynamic light scattering (DLS) at 29°C. The analysis was performed using water as the solvent (refractive index 1.3330, viscosity 0.8317 cP) and oil as the solute (refractive index 1.4000, absorption coefficient 0.0000 cm⁻¹). Measurements included d(0), d(10), d(50), d(90), and d(100) values to characterize the size distribution profile. The analysis was conducted with a total exposure time of 211 seconds using single exposure with 1000 msec exposure time length.

Cell Culture and Maintenance

MCF-7 human breast cancer cells (ATCC: HTB-22) were obtained from the National Center of Genetic Resources, Iran. Cells were cultured in DMEM medium (GIBCO™ 41965039) supplemented with 10% FBS (GIBCO-10082147) and maintained in a humidified incubator at 37°C with 5% CO₂. Medium was changed every three days, and cells were passaged upon reaching appropriate density. For passaging, cells were washed with PBS and detached using 0.25% trypsin-EDTA solution. The cell suspension was centrifuged at 300g for 5 minutes, and the resulting pellet was resuspended in fresh culture medium. Cell counting was performed using a haemocytometer with trypan blue exclusion method, and viability was assessed before experimental procedures.

Cytotoxicity Assessment

The antiproliferative effect of NE-SU was evaluated using the MTT assay. MCF-7 cells were seeded at a density of 10,000 cells per well in 96-well plates and allowed to attach for 24 hours. Cells were then treated with varying concentrations of NE-SU (20, 40, 80, 160, and 320 µg/ml) or doxorubicin (5 µM) as a positive control. After 72 hours of treatment, 100 µl of MTT solution (5 mg/ml, diluted 1:10 in culture media) was added to each well and incubated for 3-4 hours at 37°C. The supernatant was carefully removed, and formazan crystals were dissolved in 100 µl DMSO. Absorbance was measured at 570 nm using a spectrophotometer. Cell viability was calculated as a percentage relative to untreated control cells.

Apoptosis Analysis

Apoptosis was evaluated using Annexin V-FITC/PI double staining flow cytometry. Briefly, 100,000 cells were collected and suspended in 500 μ l of 1x Binding Buffer. Cells were stained with 5 μ l Annexin V-FITC and incubated for 15 minutes at 4°C in the dark. After centrifugation at 1500 RPM for 5 minutes, the supernatant was discarded, and cells were resuspended in 500 μ l Binding Buffer. Prior to analysis, 3 μ l of propidium iodide was added, and samples were analyzed using a BD-Facs Calibur flow cytometer. Data analysis was performed using FlowJo software, and statistical analysis was conducted using Prism5 software.

Animal Studies and Tumor Model Development

All animal experiments were conducted at the Research Consulting Organization (RCO) as Histogenotech brand, Pasargard Biotechnology Accelerator (Iran). Female BALB/c mice (weighing 20 \pm 2 grams) were obtained from the Laboratory Animal Center of Pasteur Institute. Animals were housed under controlled conditions with ambient temperature of 23 \pm 3°C, relative humidity of 50 \pm 10%, and alternating 12-hour light/dark cycles. Food and water were provided ad libitum throughout the experimental period. All animal procedures were conducted in accordance with institutional guidelines for the care of laboratory animals.

The breast cancer model was established by subcutaneous inoculation of 4T1 cells (1 \times 10⁵ cells in 50 μ l phosphate-buffered saline) into the right flank of each mouse. Eighteen mice were randomly divided into six groups (n=3 per group): untreated model control, NE-SU treatment groups (100 and 200 mg/kg), and doxorubicin group (20 mg/kg). Treatment was initiated after successful tumor establishment. The NE-SU groups received daily oral gavage for 30 days, while the doxorubicin group received weekly intraperitoneal injections for 4 weeks. Tumor size was measured weekly using ImageJ software.

Biochemical Analysis

Following the treatment period, animals were sacrificed and tumor tissues were collected for biochemical analysis. Oxidative stress parameters were evaluated by measuring various antioxidant enzymes. Catalase (CAT) activity was determined spectrophotometrically at 520-560 nm using a commercial assay kit. Superoxide dismutase (SOD)

activity was measured at 420 nm using the SOD assay kit, with readings taken at 0 and 2 minutes. Glutathione peroxidase (GPX) activity was assessed at 412 nm following the manufacturer's protocol. Lipid peroxidation was evaluated by measuring malondialdehyde (MDA) levels at 535 nm using the thiobarbituric acid reactive substances method.

Chemical Analysis and Antioxidant Activity Assessment

GC-MS Analysis

GC-MS analysis was performed using a Chemstation integrator system. Chromatographic separation was achieved using standardized temperature programming. Mass spectra were acquired in electron impact mode at 70 eV, and compounds were identified through library matching using WILEY275, GCDEVAL, and PMW_TOX2 databases with quality threshold \geq 90%.

DPPH Radical Scavenging Assay

The antioxidant activity was evaluated using the DPPH (2,2-Diphenyl-1-picrylhydrazyl) method. DPPH solution (7.89 mg/100 ml ethanol) was prepared and kept in dark conditions for 2 hours. The assay mixture contained 1,000 μ l DPPH solution, 800 μ l Tris-HCl buffer (pH 7.4), and 200 μ l test sample. After 30 minutes of incubation at room temperature, absorbance was measured at 517 nm. The inhibition ratio was calculated using the formula: Inhibition ratio (%) = (A1 - A2) \times 100/A1, where A1 represents the absorbance of the control and A2 the absorbance of test samples. Vitamin C served as a positive control.

Histopathological Examination

Tumor tissues were fixed in 10% neutral buffered formalin for 24-72 hours, followed by dehydration through ascending grades of ethanol (70%, 80%, 90%, and 100%, 50 minutes each). Tissues were cleared in xylene and embedded in paraffin. Sections of 5 μ m thickness were prepared using a microtome and stained with hematoxylin and eosin (H&E) following standard protocols. Stained sections were examined under a light microscope for histopathological changes and the extent of tumor necrosis.

Molecular Analysis

Gene expression analysis was performed to evaluate apoptosis-related genes. Total RNA was extracted from treated and control cells, and gene

expression levels of *BAX*, *BCL2*, and *Caspase-3* were analyzed using real-time PCR. The following primer sequences were used: h-GAPDH-F (CTTTGGTATCGTGAAGGAC) and h-GAPDH-R (GCAGGGATGATGTTCTGG) for the housekeeping gene; *h-BAX-F* (CGCCCTTTCTACTTTGACA) and *h-BAX-R* (GTGACGAGGCTTGAGGAG) for *BAX*; *h-BCL2-F* (TGGTCTTCTTTGAGTTCCGG) and *h-BCL2-R* (GGCTGTACAGTTCCACAA) for *BCL2*; and *h-Caspase3-F* (GGAAGCGAATCAATGGACTCTGG) and *h-Caspase3-R* (GCATCGACATCTGTACCAGACC) for *Caspase-3*. Gene expression was normalized to GAPDH, and relative quantification was performed using the $2^{-\Delta\Delta CT}$ method.

Antimicrobial Activity Assessment

The antimicrobial properties of NE-SU were evaluated against *Escherichia coli* (ATCC 25922) and *Pseudomonas aeruginosa* (ATCC 27853) using both minimum inhibitory concentration (MIC) and disk diffusion methods. For MIC determination, bacterial suspensions were prepared to match 0.5 McFarland standards (108 CFU/ml) and diluted 1:100. Various concentrations of NE-SU (5, 10, 20, 40, and 80 µg/ml) were tested in Mueller-Hinton broth, and bacterial growth was assessed by measuring optical density at 630 nm.

For the disk diffusion assay, sterile filter paper discs (6 mm, Whatman No. 1) were impregnated with 15 µl of the test samples and placed on Mueller-Hinton agar plates inoculated with the test organisms. After 2 hours at 4°C for diffusion, plates

were incubated at 37°C for 24 hours. Inhibition zone diameters were measured in millimeters, including the disk diameter.

Statistical Analysis

All experiments were performed in triplicate, and data are presented as mean ± standard deviation. Statistical analysis was performed using GraphPad Prism software. Comparisons between multiple groups were conducted using one-way ANALYSIS of variance (ANOVA) followed by Tukey's post-hoc test. For survival analysis, Kaplan-Meier curves were generated. Statistical significance was set at $p < 0.05$, with significance levels indicated as * $p < 0.05$, ** $p < 0.01$, *** $p < 0.001$, and **** $p < 0.0001$.

RESULTS AND DISCUSSION

Nanoemulsion Characterization

Dynamic light scattering analysis revealed that the *Selenicereus undatus* nanoemulsion (NE-SU) exhibited a bimodal size distribution with peaks at 21.2 nm and 103 nm. The particle size analysis demonstrated $d(0)$ values of 7.32/5.44/5.35 nm, $d(50)$ values of 101/23.3/21.2 nm, and $d(90)$ values of 161/96.4/33.8 nm. The temperature during measurement was maintained at 29°C, with an average count rate of 643 kcps. The size distribution curve showed good uniformity, indicating successful formulation of stable nanoemulsion particles (Fig. 1). The intensity distribution data revealed that the majority

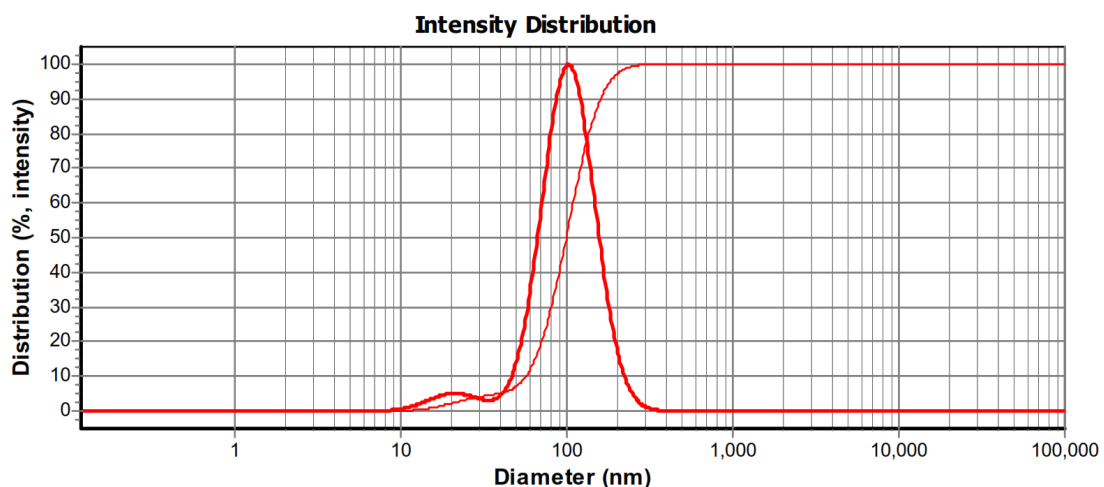


Fig. 1. Dynamic light scattering analysis of *Selenicereus undatus* nanoemulsion showing bimodal size distribution with peaks at 21.2 nm and 103 nm. The intensity distribution curve demonstrates a narrow size range with cumulative distribution indicating that 90% of particles (d_{90}) were below 161 nm, confirming the nanoscale characteristics of the formulation.

of particles fell within the nanometer range, confirming the formation of nano-sized droplets suitable for biological applications.

Morphological examination of the *Selenicereus undatus* nanoemulsion through scanning electron microscopy revealed uniformly dispersed spherical nanoparticles. The micrograph demonstrated discrete particles with diameters consistent with DLS measurements, particularly evidencing the smaller population around 20-25 nm. The particles exhibited good spatial distribution with minimal aggregation, confirming successful emulsification and formation of well-defined nanoscale structures (Fig. 2). The observed morphological characteristics validated the formation of stable nanostructures suitable for biological applications, with size distributions appropriate for cellular uptake and tissue penetration.

Cytotoxicity Assessment

The antiproliferative effects of NE-SU on MCF-7 breast cancer cells were evaluated using the MTT assay. Treatment with increasing concentrations of NE-SU (20-320 µg/ml) demonstrated a dose-dependent reduction in cell viability. After 72

hours of treatment, NE-SU at 20 µg/ml reduced cell viability to $85.81 \pm 0.65\%$, while higher concentrations of 40, 80, 160, and 320 µg/ml decreased cell viability to $61.17 \pm 1.05\%$, $51.6 \pm 0.51\%$, $46.64 \pm 1.13\%$, and $40.12 \pm 0.89\%$, respectively. The positive control doxorubicin (5 µM) showed cytotoxicity with cell viability of $55.33 \pm 2.95\%$. Statistical analysis revealed significant differences between all treatment groups compared to the control ($p < 0.0001$) (Fig. 3). The IC₅₀ value for NE-SU was calculated to be 81.09 µg/ml, indicating moderate cytotoxic potency against breast cancer cells.

Flow Cytometry Analysis

Apoptosis induction was quantified using Annexin V-FITC/PI flow cytometry. The results showed that treatment with NE-SU (80 µg/ml) induced significant apoptosis in MCF-7 cells, with an apoptotic rate of $52.11 \pm 2.092\%$ compared to $0.1083 \pm 0.1263\%$ in untreated control cells. The positive control doxorubicin (5 µM) demonstrated an apoptotic rate of $64.61 \pm 3.145\%$. The difference in apoptotic rates between NE-SU treatment and control was statistically significant ($p < 0.0001$),

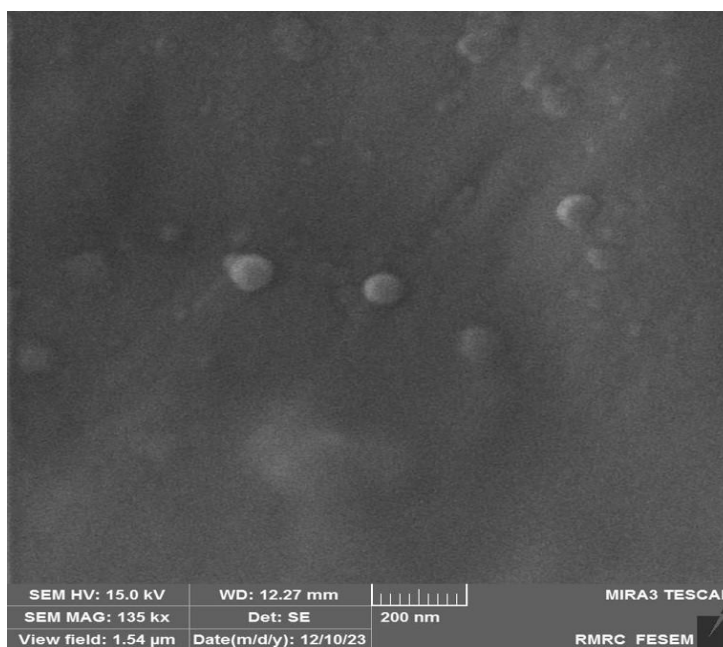


Fig. 2. Scanning electron micrograph of *Selenicereus undatus* nanoemulsion showing spherical nanoparticles with uniform size distribution. The image reveals well-dispersed particles with diameters corresponding to DLS measurements, demonstrating successful formation of stable nanoscale structures (scale bar = 200 nm).

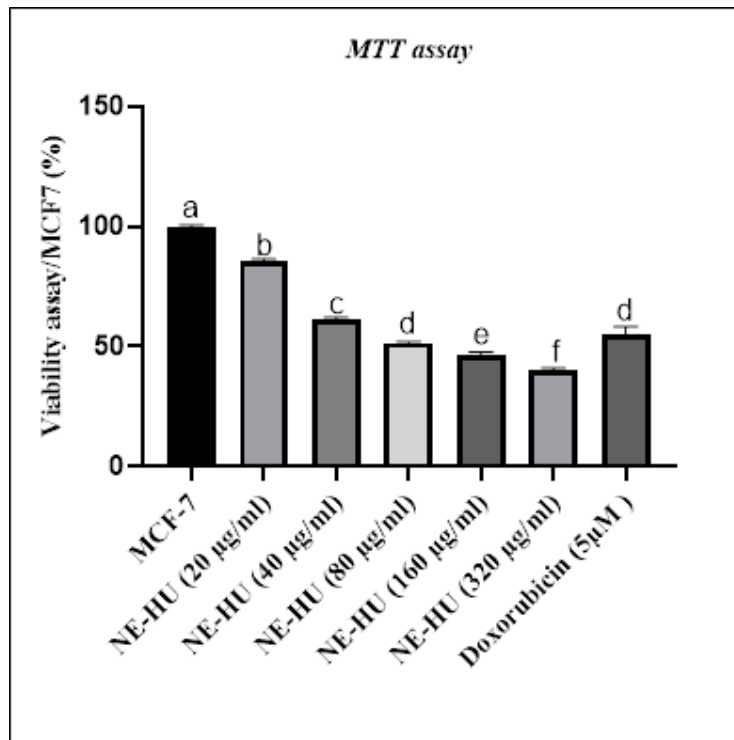


Fig. 3. Dose-dependent cytotoxic effects of *Selenicereus undatus* nanoemulsion (NE-SU) on MCF-7 breast cancer cells. Cell viability was assessed using MTT assay after 72 hours of treatment with varying concentrations of NE-SU (20-320 µg/ml) or doxorubicin (5 µM) as positive control.

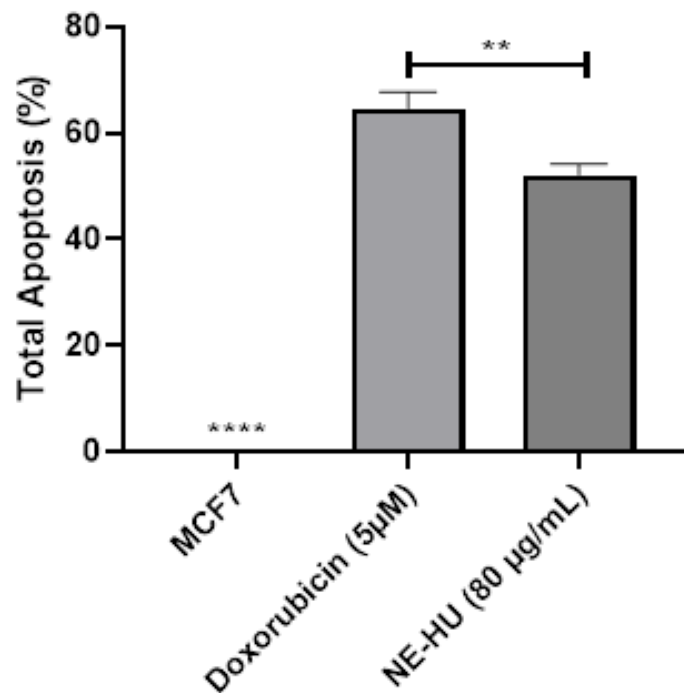


Fig. 4. Comparative analysis of apoptosis induction by *Selenicereus undatus* nanoemulsion (NE-HU) in MCF-7 breast cancer cells.

indicating potent apoptosis-inducing activity of the nanoemulsion formulation (Fig. 4).

Tumor Growth Inhibition

The therapeutic efficacy of NE-SU was evaluated in a 4T1 breast cancer mouse model over four weeks. Tumor size measurements revealed significant growth inhibition in treated groups compared to the untreated model control. At week 1, the mean tumor size in the control group was $1701 \pm 25.36 \text{ mm}^2$, while groups treated with NE-SU at 100 mg/kg and 200 mg/kg showed reduced tumor sizes of $1539 \pm 74.22 \text{ mm}^2$ and $1474 \pm 53.72 \text{ mm}^2$, respectively. The doxorubicin group (20 mg/kg) exhibited tumor size of $1417 \pm 65.73 \text{ mm}^2$.

By week 4, the antitumor effect became more pronounced, with the control group showing tumor size of $2053 \pm 86.09 \text{ mm}^2$, while NE-SU treatment at 100 mg/kg and 200 mg/kg significantly reduced tumor sizes to $1101 \pm 50.95 \text{ mm}^2$ and $834.7 \pm 31.79 \text{ mm}^2$, respectively. The doxorubicin group showed the highest tumor growth inhibition with final tumor size of $594.3 \pm 131.6 \text{ mm}^2$ (Fig. 5). Statistical analysis demonstrated significant differences between all treatment groups compared to the control ($p < 0.0001$), indicating potent antitumor activity of NE-SU in vivo.

Oxidative Stress Parameters

Analysis of antioxidant enzymes revealed significant modulation of oxidative stress markers by NE-SU treatment. Catalase (CAT) activity in tumor tissue showed marked differences between groups, with the control group showing $141.3 \pm 21.81 \text{ nM/min/mL}$, while NE-SU treatment at 80 $\mu\text{g/ml}$ increased CAT activity to $88.62 \pm 2.776 \text{ nM/}$

min/mL ($p < 0.01$). The doxorubicin group showed CAT activity of $53.96 \pm 3.791 \text{ nM/min/mL}$ (Fig. 6A).

Superoxide dismutase (SOD) activity demonstrated similar trends, with the control group showing $88.53 \pm 2.167 \text{ IU/mL}$, while NE-SU treatment significantly enhanced SOD activity to $75.69 \pm 3.409 \text{ IU/mL}$ ($p < 0.001$). The doxorubicin-treated group showed SOD activity of $49.49 \pm 2.747 \text{ IU/mL}$ (Fig. 6B). Glutathione peroxidase (GPX) activity in the control group was $1.316 \pm 0.1428 \text{ IU/mL}$, while NE-SU treatment resulted in $0.9324 \pm 0.04731 \text{ IU/mL}$ ($p < 0.01$) (Fig. 6C).

Lipid peroxidation, measured as malondialdehyde (MDA) levels, showed significant differences between groups. The control group showed MDA levels of $6.69 \pm 0.4647 \text{ }\mu\text{M/ml}$, while NE-SU treatment at 80 $\mu\text{g/ml}$ increased MDA levels to $17.36 \pm 0.9286 \text{ }\mu\text{M/ml}$ ($p < 0.001$). The doxorubicin group showed the highest MDA levels at $26.64 \pm 2.409 \text{ }\mu\text{M/ml}$, indicating increased oxidative stress (Fig. 6D).

Chemical Characterization of *S. undatus* Extract

GC-MS analysis revealed a complex phytochemical profile of the *S. undatus* extract (Fig. 7). Three major peaks were identified at retention times of 22.32, 26.73, and 30.01 minutes, representing 23.39%, 9.08%, and 67.53% of total peak area, respectively. Library matching identified tetradecanoic acid (myristic acid) with 97% similarity at 26.73 minutes and hexadecanoic acid (palmitic acid) with 99% similarity at 30.01 minutes as predominant compounds. The mass spectral fragmentation patterns showed characteristic molecular ions at m/z 228 for tetradecanoic acid and m/z 256 for hexadecanoic

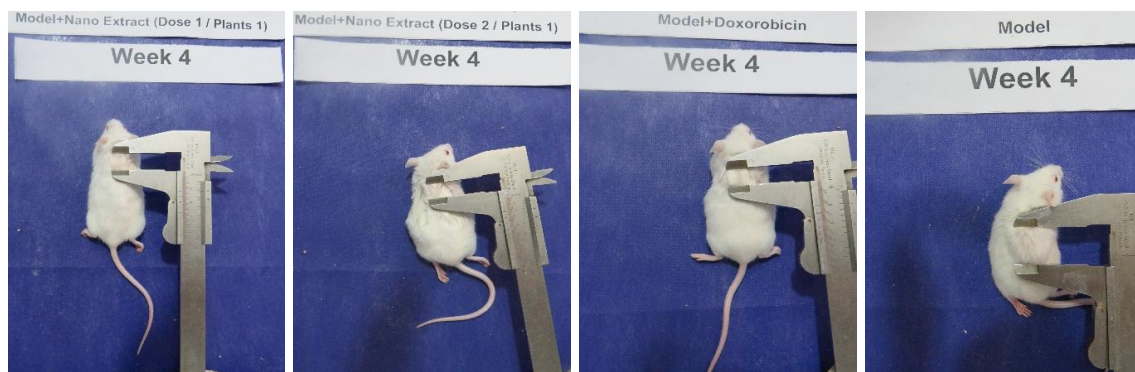


Fig. 5. Representative images demonstrating tumor size variations in BALB/c mice after 4 weeks of treatment across experimental groups.

acid, with diagnostic fragment ions supporting the structural assignments. This fatty acid composition may contribute to the formation of stable nanoemulsions and biological activities observed.

Antioxidant Activity

The free radical scavenging capacity of NE-SU was evaluated using the DPPH assay, demonstrating concentration-dependent antioxidant activity. At the lowest tested concentration (20 µg/ml), NE-SU exhibited 43.74 ± 0.8938% inhibition of DPPH radicals. The scavenging activity increased progressively with concentration, showing 57.37 ± 3.34% at 40 µg/ml, 74.7 ± 2.099% at 80 µg/ml,

93.61 ± 1.002% at 160 µg/ml, and 95.37 ± 0.6997% at 320 µg/ml. The reference antioxidant, vitamin C (30 µg/ml), demonstrated 97.5 ± 0.278% inhibition. Statistical analysis revealed significant differences between all treatment concentrations (p < 0.0001), except between the highest NE-SU concentration (320 µg/ml) and vitamin C, indicating comparable antioxidant potency at maximum concentration (Fig. 8).

Gene Expression Analysis

Real-time PCR analysis revealed significant modulation of apoptosis-related genes by NE-SU treatment. The pro-apoptotic *BAX* gene

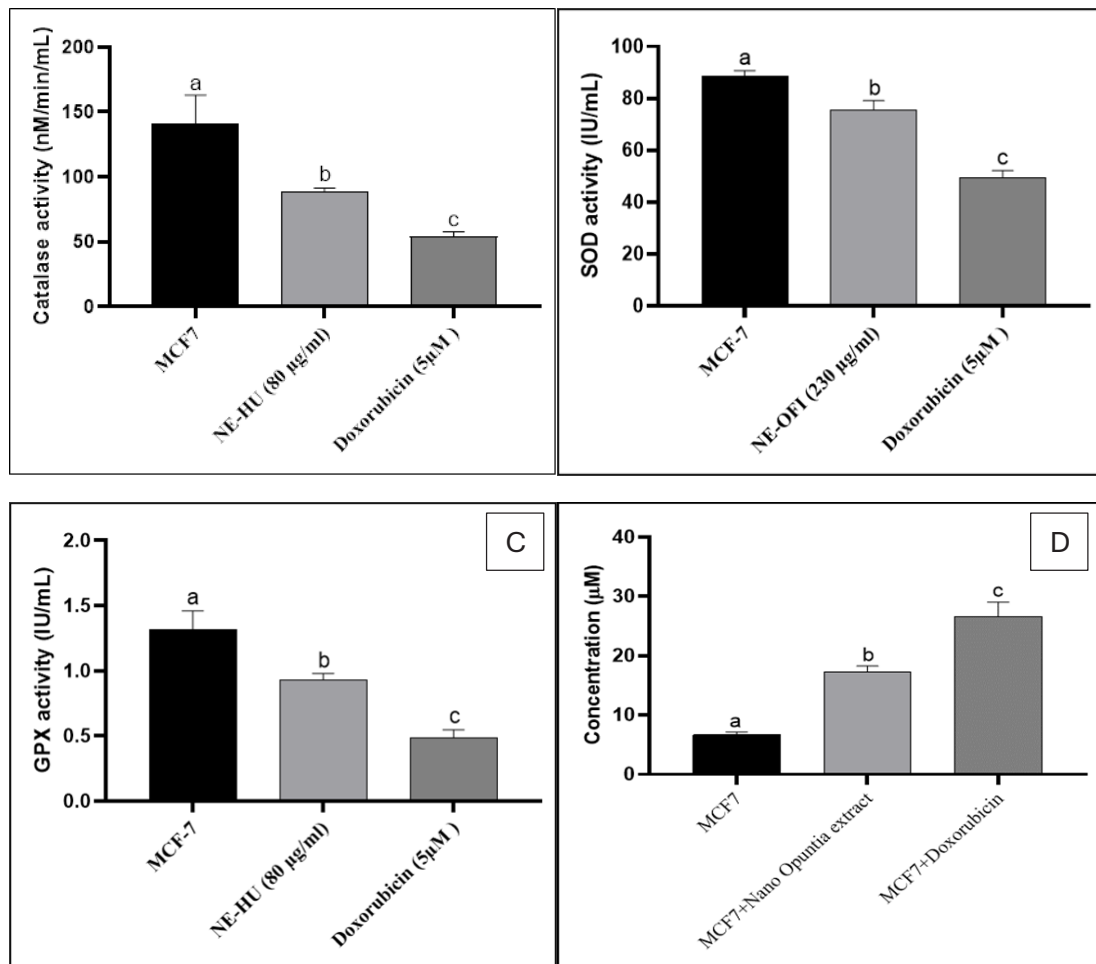


Fig. 6. Analysis of oxidative stress parameters in MCF-7 cells following treatment with NE-HU and doxorubicin. (A) Catalase (CAT) activity expressed as nM/min/mL, (B) Superoxide dismutase (SOD) activity measured in IU/mL, (C) Glutathione peroxidase (GPX) activity quantified in IU/mL, and (D) Malondialdehyde (MDA) concentration expressed in µM. Different letters (a, b, c) indicate statistically significant differences between groups as determined by one-way ANOVA followed by Tukey's post-hoc test (p < 0.01). Data are presented as mean ± SD from three independent experiments. MCF-7: untreated control; NE-HU: *Selenicereus undatus* nanoemulsion at 80 µg/ml; Doxorubicin: positive control at 5 µM.

showed significant upregulation in treated groups compared to control. NE-SU treatment at 80 µg/ml increased *BAX* expression by 3.519 ± 0.4088 fold compared to control (normalized to 1.004 ± 0.1046). The doxorubicin-treated group showed the highest *BAX* upregulation at 8.524 ± 1.254 fold ($p < 0.0001$) (Fig. 9A).

Conversely, the anti-apoptotic *BCL2* gene showed significant downregulation following treatment. The control group expression was normalized to 1.007 ± 0.1468 , while NE-SU treatment reduced *BCL2* expression to 0.3208 ± 0.06353 fold. Doxorubicin treatment resulted in the lowest *BCL2* expression at 0.1149 ± 0.005286 fold ($p < 0.001$) (Fig. 9B). The *BAX/BCL2* ratio, an important indicator of apoptotic potential, was significantly increased in all treatment groups.

Caspase-3 expression, a key marker of apoptosis execution, was significantly enhanced by NE-SU treatment. Compared to control

(normalized to 1.001 ± 0.06337), NE-SU increased *Caspase-3* expression by 2.343 ± 0.06203 fold, while doxorubicin treatment resulted in 3.78 ± 0.4198 fold increase ($p < 0.0001$) (Fig. 9C). These molecular findings corroborate the apoptosis-inducing effects observed in flow cytometry analysis.

Histopathological Examination

Microscopic examination of H&E-stained tumor sections revealed significant histological changes in treated groups compared to control (Fig. 10). The control group showed densely packed tumor cells with minimal necrosis ($7.157 \pm 1.773\%$ necrotic area). Treatment with NE-SU at 100 mg/kg and 200 mg/kg showed increased areas of tumor necrosis ($14.64 \pm 3.476\%$ and $36.62 \pm 5.828\%$, respectively). The doxorubicin-treated group exhibited the highest degree of tumor necrosis at $49.95 \pm 6.446\%$. Statistical

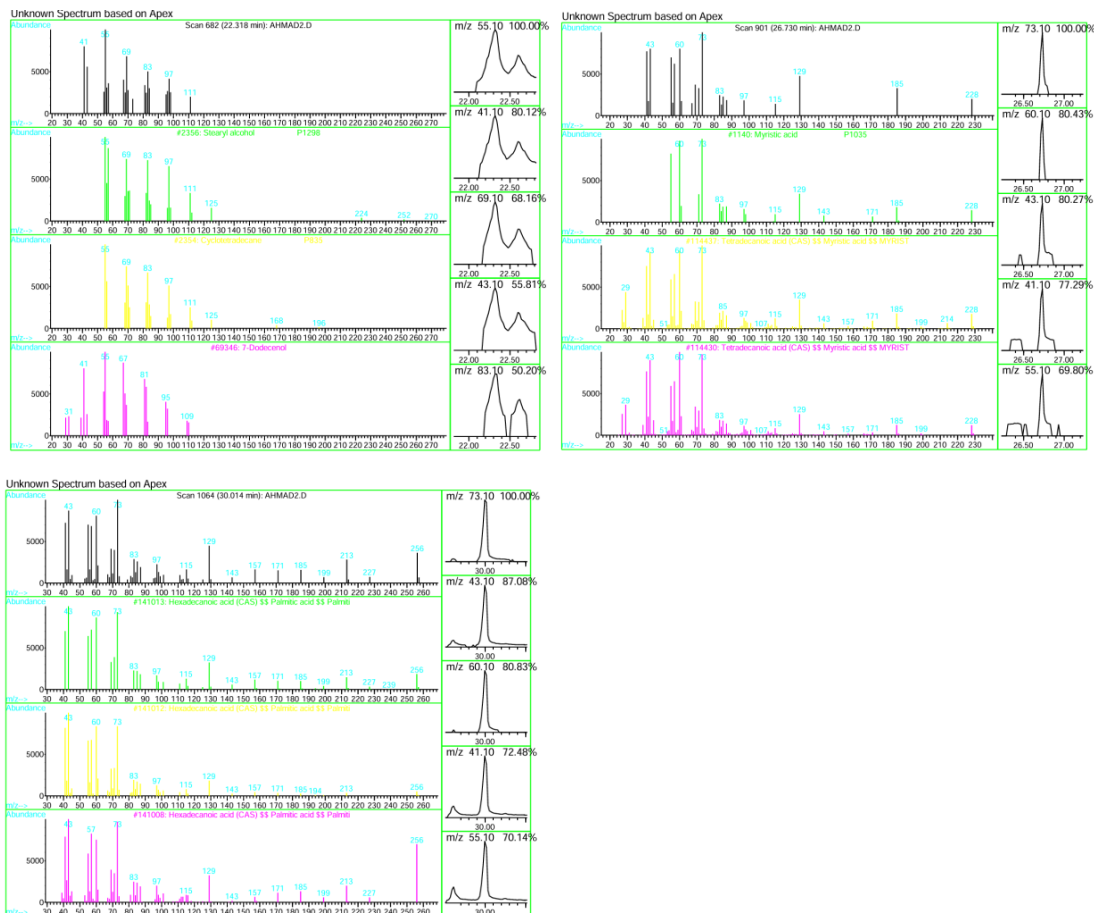


Fig. 7. GC-MS spectral analysis and mass fragmentation patterns of *Selenicereus undatus* extract constituents.

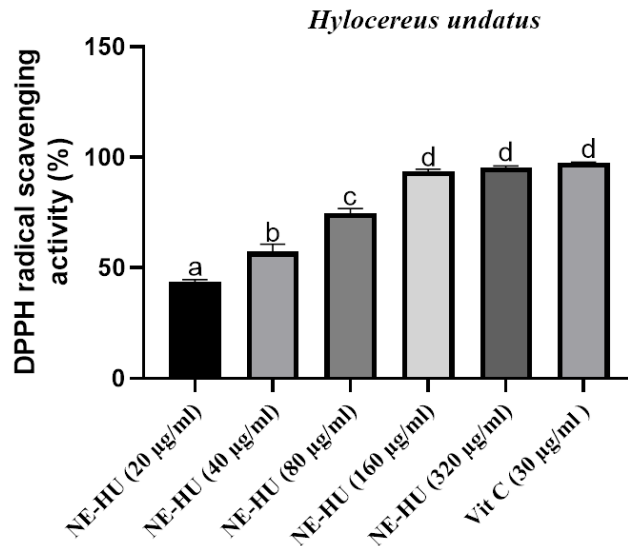


Fig. 8. DPPH radical scavenging activity of *Selenicereus undatus* nanoemulsion (NE-HU). Concentration-dependent antioxidant activity was evaluated using DPPH assay. Different concentrations of NE-HU (20-320 µg/mL) were compared with vitamin C (30 µg/mL) as positive control. Different letters (a-d) indicate statistically significant differences between groups ($p < 0.01$) as determined by one-way ANOVA followed by Tukey's post-hoc test. Data represent mean \pm SD from three independent experiments.

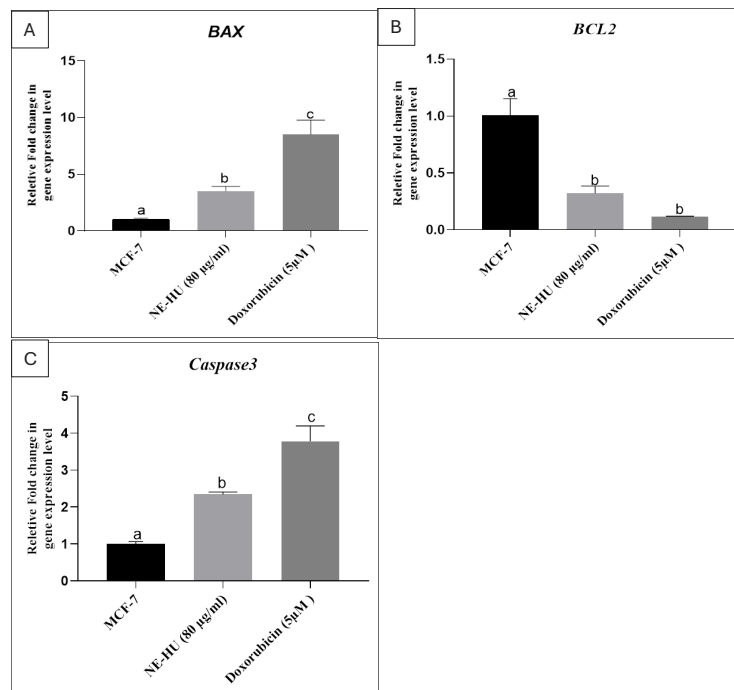


Fig. 9. Expression analysis of apoptosis-related genes in MCF-7 cells following treatment. Relative mRNA expression levels of (A) *BAX*, (B) *BCL2*, and (C) *Caspase-3* were analyzed by real-time PCR. Gene expression was normalized to GAPDH and presented as fold change relative to untreated control. Different letters indicate statistically significant differences between groups ($p < 0.01$). Data represent mean \pm SD from three independent experiments.

analysis showed significant differences in necrotic areas between all treatment groups ($p < 0.001$), indicating the effectiveness of NE-SU in inducing tumor cell death (Fig. 11).

Antimicrobial Activity

The antimicrobial potential of NE-SU was evaluated using both minimum inhibitory concentration (MIC) and disk diffusion methods against two clinically relevant bacterial strains. The MIC assay results demonstrated concentration-dependent growth inhibition of both tested

organisms. Against *Escherichia coli* ATCC 25922, NE-SU showed progressive growth inhibition with increasing concentrations. The optical density measurements at 630 nm revealed that at 5 $\mu\text{g/ml}$, the bacterial growth ($\text{OD} = 1.106 \pm 0.002646$) was minimally affected compared to control ($\text{OD} = 1.867 \pm 0.0692$). However, at higher concentrations of 40 $\mu\text{g/ml}$ and 80 $\mu\text{g/ml}$, significant growth inhibition was observed with OD values of 0.8263 ± 0.004509 and 0.812 ± 0.01136 , respectively ($p < 0.0001$) (Fig. 12A).

Similar antimicrobial effects were observed

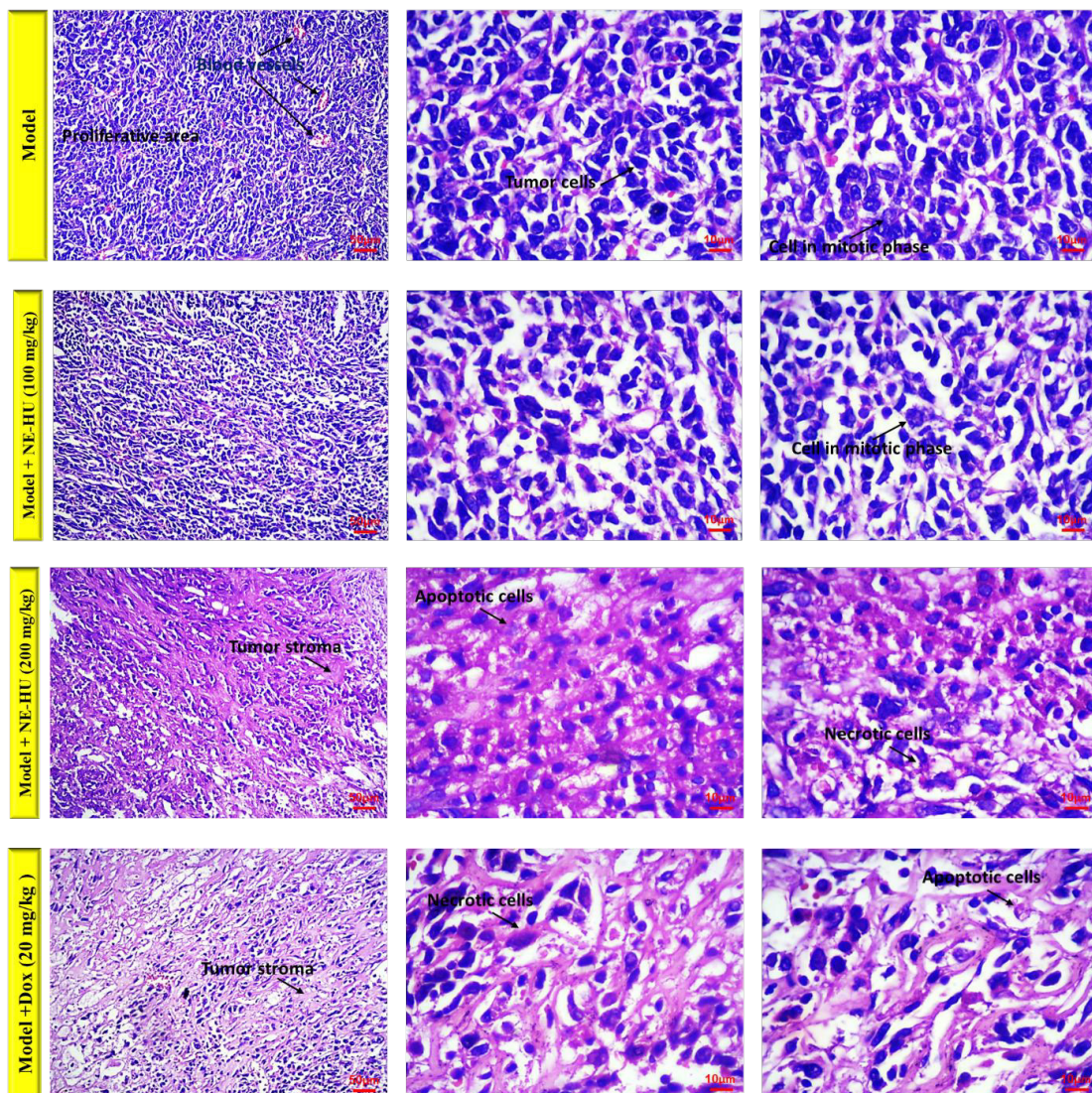


Fig. 10. Histopathological examination of breast cancer tissue sections. Representative photomicrographs of H&E-stained tumor sections (scale bar = 40 μm) showing morphological changes in untreated model control, Doxorubicin treated group and NE-HU treated groups at different magnifications. Images demonstrate proliferative areas, tumor cell characteristics, and mitotic phases in both groups.

against *Pseudomonas aeruginosa* ATCC 27853. The control group showed an OD of 1.907 ± 0.00724 , while treatment with NE-SU at $40 \mu\text{g/ml}$ and $80 \mu\text{g/ml}$ reduced bacterial growth to OD values of 0.8293 ± 0.004041 and 0.8187 ± 0.001528 , respectively. Statistical analysis revealed significant differences between all treatment concentrations compared to control ($p < 0.0001$), indicating broad-spectrum antibacterial activity of the nanoemulsion (Fig. 12B).

The disk diffusion assay provided complementary evidence of antimicrobial activity. NE-SU demonstrated consistent inhibition zones against both bacterial strains. The zone of inhibition measured 4 mm for both *E. coli* and *P. aeruginosa*, suggesting moderate antibacterial activity. While these zones were smaller compared to standard antibiotics, they indicate the potential utility of NE-SU as an antimicrobial agent, particularly considering its natural origin and the advantages of the nanoemulsion formulation.

These findings collectively demonstrate that NE-SU possesses notable antimicrobial properties against both Gram-negative bacterial strains

tested, suggesting its potential application not only as an anticancer agent but also as an antimicrobial compound. The dual therapeutic potential of NE-SU could be particularly beneficial in preventing secondary bacterial infections during cancer treatment.

The present study demonstrates the multifaceted therapeutic potential of *Selenicereus undatus* nanoemulsion (NE-SU) against breast cancer through various mechanisms of action. These findings contribute to the growing body of evidence supporting the use of nanoemulsion-based delivery systems for natural compounds in cancer therapy, while also revealing novel insights into molecular mechanisms and therapeutic applications.

This successful development of a stable nanoemulsion with bimodal size distribution (21.2 nm and 103 nm) in this study represents a significant advancement in drug delivery technology. This size range aligns with recent findings by Tarik Alhamdany *et al.* (2021), who demonstrated optimal therapeutic efficacy with nanoemulsions in the 80-100 nm range

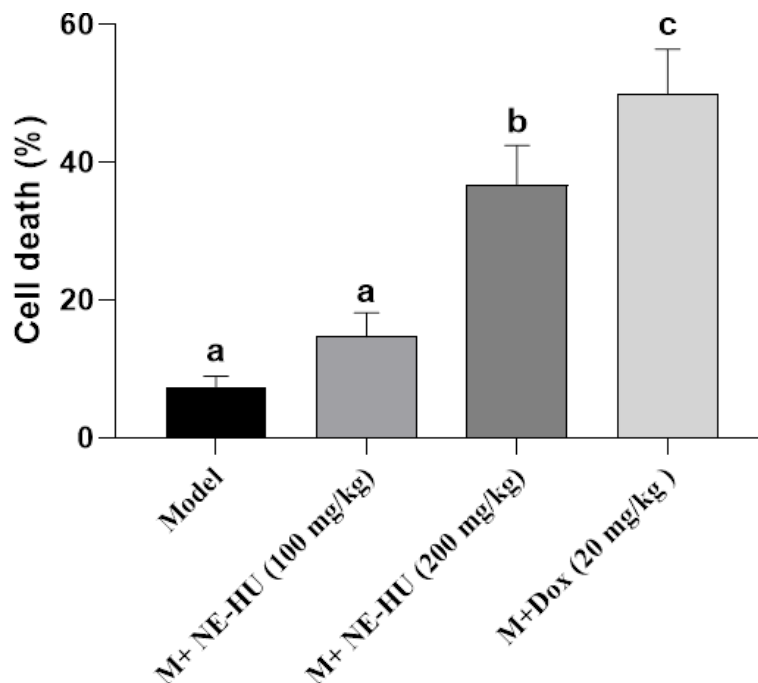


Fig. 11. Quantitative analysis of cell death in breast cancer tissue following treatment. Comparative analysis of cell death percentages in tumor tissue from different treatment groups: untreated model control, NE-HU at two doses (100 and 200 mg/kg), and doxorubicin (20 mg/kg). Different letters (a-c) indicate statistically significant differences between groups ($p < 0.01$). Data represent mean \pm SD ($n=3$ per group).

for breast cancer applications [23]. The stability characteristics of studied formulation are particularly noteworthy when compared to other recent nanoemulsion developments. Fardous *et al.* (2021) reported that gel-in-water nanoemulsions with mean diameters around 206 nm showed high drug loading efficiency ($\approx 97\%$), suggesting that the bimodal distribution of current research might offer advantages in terms of both stability and cellular uptake [24].

The choice of surfactants and co-surfactants in the formulation of this study was informed by recent advances in the field. This is supported by Kotta *et al.* (2022), who demonstrated that careful optimization of surfactant levels and homogenization parameters is crucial for developing effective thermosensitive nanoemulsions. This research approach to formulation optimization parallels recent work by Yadav *et al.* (2023), who successfully employed a Quality by Design (QbD) approach to optimize nanoemulsion characteristics for enhanced therapeutic efficacy [25].

The cytotoxicity profile of NE-SU against MCF-7 cells ($IC_{50} = 81.09 \mu\text{g/ml}$) demonstrates significant therapeutic potential while maintaining a favorable safety profile.

The modulation of oxidative stress parameters reveals a complex interaction with cellular redox systems. These findings show significant alterations

in antioxidant enzyme activities, particularly changes in CAT, SOD, and GPX levels. This aligns with recent work by Guneidy *et al.* (2023), who demonstrated that natural compounds can effectively modulate the glutathione cycle and antioxidant enzyme systems in breast cancer cells [26]. The increase in MDA levels (from 6.69 to 17.36 $\mu\text{M/ml}$) indicates enhanced lipid peroxidation, which could contribute to cancer cell death while maintaining a potentially less toxic profile compared to conventional chemotherapeutics.

The molecular analysis of apoptosis-related genes provides crucial mechanistic insights, with significant upregulation of *BAX* (3.519-fold) and downregulation of *BCL2* (0.3208-fold). This modulation pattern aligns with recent findings by Zhang *et al.* (2021) on physcion's anti-breast cancer properties, where similar alterations in the *BAX/BCL2* ratio were observed [27]. The marked increase in *Caspase-3* expression (2.343-fold) further validates the activation of the apoptotic cascade, consistent with the mechanisms reported by Hassanshahi *et al.* (2022) in their investigation of natural compound-induced apoptosis in breast cancer models [28].

The *in vivo* studies provided compelling evidence for therapeutic efficacy, with approximately 59% tumor growth inhibition in the high-dose group (200 mg/kg). This level of tumor suppression compares favorably with recent findings by Li *et al.* (2023),

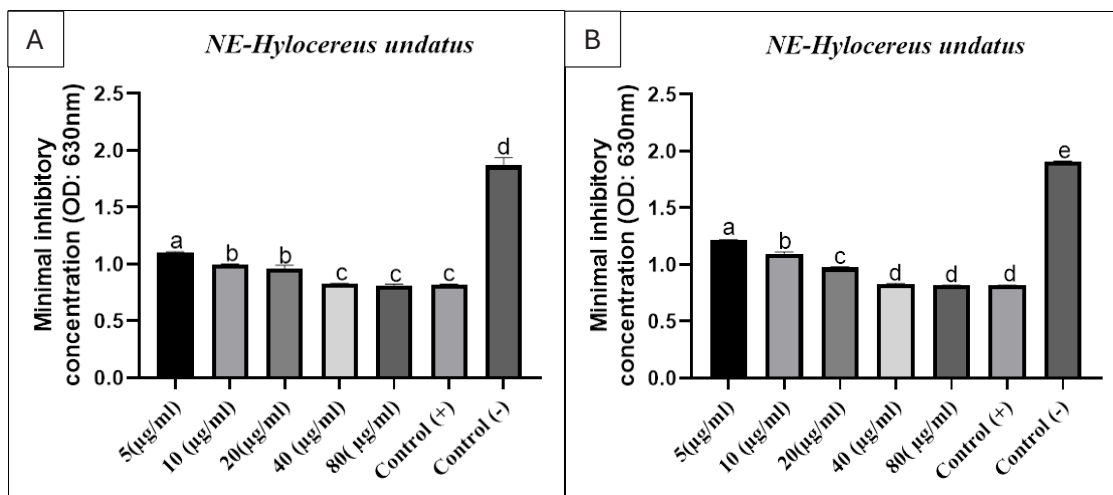


Fig. 12. Minimal inhibitory concentration analysis of NE-HU against bacterial growth. (A) *Escherichia coli*, (B) *Pseudomonas aeruginosa*. Antimicrobial activity was assessed by measuring optical density at 630 nm across different concentrations of NE-HU (5-80 $\mu\text{g/ml}$). Different letters (a-d) indicate statistically significant differences between groups ($p < 0.01$). Data represent mean \pm SD from three independent experiments.

who observed a 60.5% reduction in tumor weight within two weeks using plant-derived compounds [29]. The progressive reduction in tumor size over the four-week treatment period demonstrates sustained antitumor activity, suggesting effective bioavailability of the nanoemulsion formulation.

The findings of this research regarding tumor necrosis and histopathological changes are particularly noteworthy when considered alongside recent work by Kaur *et al.* (2022), who demonstrated similar efficacy using frankincense oil-loaded nanoemulsions [30]. The combined evidence suggests that properly formulated natural compound nanoemulsions can achieve therapeutic outcomes comparable to conventional chemotherapeutics while potentially offering improved safety profiles.

The demonstrated antimicrobial activity against both *E. coli* and *P. aeruginosa* represents an important secondary benefit of NE-SU treatment. The observed zones of inhibition (4 mm) and significant growth reduction at concentrations above 40 µg/ml align with findings from Safdar *et al.* (2023), who reported similar antimicrobial efficacy for *S. undatus* extracts [31]. This dual therapeutic potential – combining anticancer and antimicrobial effects – could be particularly valuable in clinical settings where secondary infections during cancer treatment are a concern.

The collective findings suggest several promising directions for future research and development. The enhanced bioavailability through nanoemulsion formulation, coupled with multiple mechanisms of action, positions NE-SU as a potential candidate for combination therapy. Recent work by Fu *et al.* (2022) on CBD-based nanotherapeutics demonstrates the potential for such natural compound-based treatments to achieve high tumor inhibition rates (>80%) with good tolerability [32].

Several areas warrant further investigation

First, the potential for synergistic interactions between NE-SU and conventional chemotherapeutics should be explored, similar to the approach taken by Choi *et al.* (2020) with oxaliplatin-loaded nanoemulsions [33]. Their successful demonstration of enhanced antitumor efficacy through oral delivery suggests similar possibilities for the current formulation.

Second, detailed pharmacokinetic studies would be valuable for optimizing dosing regimens.

The work of Fofaria *et al.* (2016) with piplartine nanoemulsions provides a useful model for such investigations, demonstrating how nanoemulsion formulation can enhance oral bioavailability by up to 1.5-fold [34].

Third, investigation of effects on resistant cell lines and other cancer types could broaden the therapeutic applications. Recent reviews by Chen *et al.* (2021) on natural products against triple-negative breast cancer suggest that natural compound-based nanotherapeutics might be particularly valuable for treating resistant cancer phenotypes [35].

Limitations and Considerations

While the findings of this study are promising, several limitations should be acknowledged. The use of a single cancer cell line and animal model, while providing proof of concept, may not fully represent the heterogeneity of breast cancer in clinical settings.

Additionally, longer-term safety studies would be needed to fully establish the therapeutic window and potential cumulative toxicities. The work of Miron *et al.* (2017) on flavonoid modulators of metabolic enzymes and drug transporters suggests that careful consideration of potential drug interactions will be crucial for clinical development [36].

CONCLUSION

This comprehensive investigation demonstrates that *Selenicereus undatus* nanoemulsion (NE-SU) represents a promising therapeutic approach for breast cancer treatment through multiple mechanisms of action. The successful development of a stable nanoemulsion with optimal bimodal size distribution (21.2 nm and 103 nm) achieved significant therapeutic outcomes while maintaining favorable safety profiles. The formulation demonstrated potent cytotoxicity against MCF-7 breast cancer cells with an IC50 of 81.09 µg/ml, while flow cytometry analysis confirmed substantial apoptosis induction (52.11 ± 2.092%) at 80 µg/ml.

In vivo studies provided compelling evidence of therapeutic efficacy, with approximately 59% tumor growth inhibition in the high-dose group (200 mg/kg). The molecular analyses revealed significant modulation of apoptosis-related genes, with marked upregulation of pro-apoptotic *BAX* (3.519-fold) and downregulation of anti-apoptotic

BCL2 (0.3208-fold), confirming the mechanistic basis of the observed therapeutic effects. Furthermore, the demonstrated antimicrobial activity against both *E. coli* and *P. aeruginosa* suggests potential additional benefits in managing secondary complications during cancer treatment.

The observed effects on oxidative stress parameters and gene expression profiles provide valuable insights into the mechanism of action, while histopathological findings confirm the therapeutic efficacy through increased tumor necrosis. While these results are promising, further research is warranted to fully characterize the long-term safety profile and potential interactions with conventional chemotherapeutics. Additionally, investigation of effects across different cancer types and resistant cell lines could expand the therapeutic applications of this approach.

This study establishes NE-SU as a viable candidate for breast cancer therapy, offering a novel treatment modality that combines multiple therapeutic benefits with potentially reduced adverse effects. The findings contribute significantly to the growing body of evidence supporting the use of nanoemulsion-based delivery systems for natural compounds in cancer therapy and provide a foundation for future clinical investigations.

ACKNOWLEDGEMENTS

We would like to thank Urmia University for funding this project, the Babylon University for providing some of laboratory equipment and facilities and dear people who helped us in carrying out this research.

CONFLICT OF INTEREST

The authors declare that there is no conflict of interests regarding the publication of this manuscript.

REFERENCES

1. Sung H, Ferlay J, Siegel RL, Laversanne M, Soerjomataram I, Jemal A, et al. Global Cancer Statistics 2020: GLOBOCAN Estimates of Incidence and Mortality Worldwide for 36 Cancers in 185 Countries. *CA Cancer J Clin.* 2021;71(3):209-249.
2. Bray F, Laversanne M, Sung H, Ferlay J, Siegel RL, Soerjomataram I, et al. Global cancer statistics 2022: GLOBOCAN estimates of incidence and mortality worldwide for 36 cancers in 185 countries. *CA Cancer J Clin.* 2024;74(3):229-263.
3. Wilkinson L, Gathani T. Understanding breast cancer as a global health concern. *The British Journal of Radiology.* 2021;95(1130).
4. Obidiro O, Battogtokh G, Akala EO. Triple Negative Breast Cancer Treatment Options and Limitations: Future Outlook. *Pharmaceutics.* 2023;15(7):1796.
5. Won KA, Spruck C. Triple-negative breast cancer therapy: Current and future perspectives (Review). *Int J Oncol.* 2020;57(6):1245-1261.
6. Rawat PS, Jaiswal A, Khurana A, Bhatti JS, Navik U. Doxorubicin-induced cardiotoxicity: An update on the molecular mechanism and novel therapeutic strategies for effective management. *Biomedicine & Pharmacotherapy.* 2021;139:111708.
7. Shah K, Chen J, Chen J, Qin Y. Pitaya Nutrition, Biology, and Biotechnology: A Review. *Int J Mol Sci.* 2023;24(18):13986.
8. Wu X, Wang Y, Huang X-J, Fan C-L, Wang G-C, Zhang X-Q, et al. Three new glycosides from *Hylocereus undatus*. *J Asian Nat Prod Res.* 2011;13(8):728-733.
9. Tang W, Li W, Yang Y, Lin X, Wang L, Li C, et al. Phenolic Compounds Profile and Antioxidant Capacity of Pitahaya Fruit Peel from Two Red-Skinned Species (*Hylocereus polyrhizus* and *Hylocereus undatus*). *Foods.* 2021;10(6):1183.
10. Chen S-Y, Xu C-Y, Mazhar MS, Naiker M. Nutritional Value and Therapeutic Benefits of Dragon Fruit: A Comprehensive Review with Implications for Establishing Australian Industry Standards. *Molecules.* 2024;29(23):5676.
11. Liao W, Liu W, Yan Y, Li L, Tong J, Huang Y, et al. *Hylocereus undatus* flower extract suppresses OVA-induced allergic asthma in BALB/c mice by reducing airway inflammation and modulating gut microbiota. *Biomedicine and Pharmacotherapy.* 2022;153:113476.
12. Manzari-Tavakoli A, Babajani A, Tavakoli MM, Safaeinejad F, Jafari A. Integrating natural compounds and nanoparticle-based drug delivery systems: A novel strategy for enhanced efficacy and selectivity in cancer therapy. *Cancer Medicine.* 2024;13(5).
13. Preeti, Sambhakar S, Malik R, Bhatia S, Al Harrasi A, Rani C, et al. Nanoemulsion: An Emerging Novel Technology for Improving the Bioavailability of Drugs. *Scientifica.* 2023;2023:1-25.
14. Nieto Marín V, Buccini DF, Gomes da Silva V, Fernandez Soliz IA, Franco OL. Nanoformulations of bioactive compounds derived from essential oils with antimicrobial activity. *Nano Trends.* 2025;9:100070.
15. Kaur G, Panigrahi C, Agarwal S, Khuntia A, Sahoo M. Recent trends and advancements in nanoemulsions: Production methods, functional properties, applications in food sector, safety and toxicological effects. *Food Physics.* 2024;1:100024.
16. Nakamura Y, Mochida A, Choyke PL, Kobayashi H. Nanodrug Delivery: Is the Enhanced Permeability and Retention Effect Sufficient for Curing Cancer? *Bioconjugate Chemistry.* 2016;27(10):2225-2238.
17. Martínez-Ballesta M, Gil-Izquierdo Á, García-Viguera C, Domínguez-Perles R. Nanoparticles and Controlled Delivery for Bioactive Compounds: Outlining Challenges for New "Smart-Foods" for Health. *Foods.* 2018;7(5):72.
18. Bukowski K, Kciuk M, Kontek R. Mechanisms of Multidrug Resistance in Cancer Chemotherapy. *Int J Mol Sci.* 2020;21(9):3233.
19. Ajith AK, Subramani S, Manickam AH, Ramasamy S. Chemotherapeutic Resistance Genes of Breast Cancer Patients – An Overview. *Advanced Pharmaceutical Bulletin.*

- 2021.
20. Ezike TC, Okpala US, Onoja UL, Nwike CP, Ezeako EC, Okpara OJ, et al. Advances in drug delivery systems, challenges and future directions. *Heliyon*. 2023;9(6):e17488.
 21. Delgado A, Guddati AK. Infections in Hospitalized Cancer Patients. *World J Oncol*. 2021;12(6):195-205.
 22. Mao X, Wu S, Huang D, Li C. Complications and comorbidities associated with antineoplastic chemotherapy: Rethinking drug design and delivery for anticancer therapy. *Acta Pharmaceutica Sinica B*. 2024;14(7):2901-2926.
 23. Tarik Alhamdany A, Saeed AMH, Alaayedi M. Nanoemulsion and Solid Nanoemulsion for Improving Oral Delivery of a Breast Cancer Drug: Formulation, Evaluation, and a Comparison Study. *Saudi Pharmaceutical Journal*. 2021;29(11):1278-1288.
 24. Fardous J, Omoso Y, Joshi A, Yoshida K, Patwary MKA, Ono F, et al. Development and characterization of gel-in-water nanoemulsion as a novel drug delivery system. *Materials Science and Engineering: C*. 2021;124:112076.
 25. Yadav PK, Saklani R, Tiwari AK, Verma S, Chauhan D, Yadav P, et al. Ratiometric codelivery of Paclitaxel and Baicalein loaded nanoemulsion for enhancement of breast cancer treatment. *Int J Pharm*. 2023;643:123209.
 26. Guneidy RA, Zaki ER, Karim GSAA, Saleh NS, Shokeer A. Adverse effect of *Tamarindus indica* and tamoxifen combination on redox balance and genotoxicity of breast cancer cell. *Journal of Genetic Engineering and Biotechnology*. 2023;21(1):131.
 27. Zhang L, Dong R, Wang Y, Wang L, Zhou T, Jia D, et al. The anti-breast cancer property of physcion via oxidative stress-mediated mitochondrial apoptosis and immune response. *Pharm Biol*. 2021;59(1):301-308.
 28. Hassanshahi J, Hajjalizadeh Z, Niknia S, Mahmoodi M, Kaeidi A. Anti-tumor effects of *Thymus Caramanicus* Jales extract in mice through oxidative stress, inflammation and apoptosis. *Journal of Pharmacy and Pharmacology*. 2022;74(12):1797-1804.
 29. Li Y, Ma NL, Chen H, Zhong J, Zhang D, Peng W, et al. Corrigendum to "High-throughput screening of ancient forest plant extracts shows cytotoxicity towards triple-negative breast cancer" [*Environ. Int.* 181 (2023) 108279]. *Environ Int*. 2024;187:108695.
 30. Kaur H, Kaur K, Singh A, Bedi N, Singh B, Alturki MS, et al. Frankincense oil-loaded nanoemulsion formulation of paclitaxel and erucin: A synergistic combination for ameliorating drug resistance in breast cancer: In vitro and in vivo study. *Front Pharmacol*. 2022;13.
 31. Safdar S, Shamim S, Khan M, Imran A, Khan MA, Ali Q, et al. Probing Antibacterial and Anticancer Potential of *Selenicereus undatus*, *Pistacia vera* L. and *Olea europaea* L. against Uropathogens, MCF-7 and A2780 Cancer Cells. *Molecules*. 2023;28(24):8148.
 32. Fu J, Zhang K, Lu L, Li M, Han M, Guo Y, et al. Improved Therapeutic Efficacy of CBD with Good Tolerance in the Treatment of Breast Cancer through Nanoencapsulation and in Combination with 20(S)-Protopanaxadiol (PPD). *Pharmaceutics*. 2022;14(8):1533.
 33. Choi JU, Maharjan R, PANGENI R, Jha SK, Lee NK, Kweon S, et al. Modulating tumor immunity by metronomic dosing of oxaliplatin incorporated in multiple oral nanoemulsion. *Journal of Controlled Release*. 2020;322:13-30.
 34. Fofaria NM, Qhattal HSS, Liu X, Srivastava SK. Nanoemulsion formulations for anti-cancer agent piplartine—Characterization, toxicological, pharmacokinetics and efficacy studies. *Int J Pharm*. 2016;498(1-2):12-22.
 35. Chen H, Yang J, Yang Y, Zhang J, Xu Y, Lu X. The Natural Products and Extracts: Anti-Triple-Negative Breast Cancer in Vitro. *Chemistry & Biodiversity*. 2021;18(7).
 36. Miron A, Aprotosoae AC, Trifan A, Xiao J. Flavonoids as modulators of metabolic enzymes and drug transporters. *Annals of the New York Academy of Sciences*. 2017;1398(1):152-167.